CFD Investigation of Solar Air Heater by varying Rib Profiles

Manoj Kumar Darwai[1] Mr. Jagdeesh Saini[2]
[1]Research Student [2]Assistant Professor
[1,2]Department of Mechanical Engineering
[1,2]B. M. College of Technology, Indore, India

Abstract— Enhancement of heat transfer rate is important factor in order to improve performance solar air heater. This enhancement is possible by means of incorporating artificial roughness. The effect of artificial roughness is studied using CFD. The analysis software used is ANSYS CFX. Artificial roughness is used in one side wall of solar air heater absorber plate to break laminar boundary sub layer. It enhances rate of heat transfer from the absorber plate to flow of air stream. The artificial roughness is varied with different (P/E) ratio at various Reynolds number. Outlet temperature, heat transfer rate and Nusselt number is computed.

Key words: Solar Air Heater, CFD, Artificial Roughness, Thermal Efficiency, ANSYS-CFX

I. INTRODUCTION

It is an effective technique to use artificial roughness in the form of repeated ribs on a surface to augment the heat transfer rate. Augmentation of convective heat transfer of a rectangular duct with the help of ribs is now common between engineers and scientists. This concept is widely applied in enhancing the thermo-hydraulic efficiency of various industrial applications such as solar air heaters, air conditioning components, refrigerators, chemical processing plants, automobile radiators and. Solar air heater is a device used to augment the temperature of air with the help of heat extracted from solar energy. These are cheap, have simple design, require less maintenance and are eco-friendly. As a result, they have major applications in seasoning of timber, drying of agricultural products, space heating, curing of clay/concrete building components and curing of industrial products.

The shape of a solar air heater of conventional application is that of rectangular duct having an absorber plate at the top, a rear plate, insulated wall under the rear plate, a glass cover over the sun-radiation exposed surface, and a passage between the bottom plate and absorber for air to flow in. The detailed constructional details of a solar air heater are shown in fig. 1.

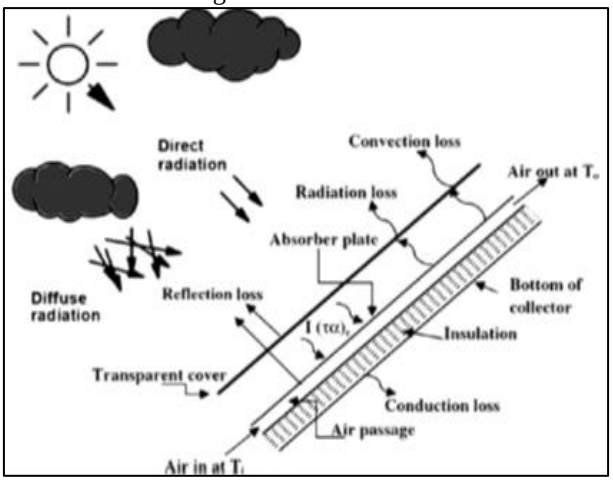

Fig. 1: Solar air heater constructional details

II. LITERATURE SURVEY

Vipin B. Gawande, Dhoble A. S., Zodpe D. B., Sunil Chamoli, (2015) has performed an experimental and two-dimensional computational fluid dynamics (CFD) analysis of a solar air heater using reverse L shape rib as artificial roughness on the absorber plate. The relative roughness pitch (P/e=7.14–17.86), Reynolds number (Re = 3800–18,000) and relative roughness height (e/D = 0.042) are chosen as design variables for analysis. The relative roughness pitch of 7.14 provides best thermo-hydraulic performance of 1.90 considering the maximum heat transfer.

Vipin B. Gawande, Dhoble A. S., Zodpe D. B., Sunil Chamoli, (2015) has performed an experimental and two-dimensional computational fluid dynamics (CFD) analysis of a solar air heater using chamfered square rib as artificial roughness on the absorber plate. The relative roughness pitch (P/e=7.14–17.86), chamfer angle (α = 0°– 40°), Reynolds number (Re = 3800–18,000) and relative roughness height (e/D = 0.042) are chosen as design variables for analysis. The chamfer angle of 20° on square rib and relative roughness pitch of 7.14 provide best thermo-hydraulic performance of 2.047 considering the maximum heat transfer and minimum pressure drop.

Anil Singh Yadav, (2013) has done the performance analysis of transverse rectangular rib on CFD ANSYS FLUENT 15 and found that the maximum enhancement of average Nusselt number is found to be 2.86 times that of smooth duct for relative roughness pitch of 7.14, relative roughness height of 0.042 and for Reynolds no. 15000.

Anil Singh Yadav, Bhagoria J.L., (2013) has done the performance analysis of small diameter circular rib on CFD ANSYS FLUENT 15 and found that the maximum enhancement of average Nusselt number is found to be 2.31 times that of smooth duct for relative roughness pitch of 7.14 and for relative roughness height of 0.042. Results were validated by comparing with available experimental results and the discrepancy between available experimental data and computational results were less than 7.5%.

J.L. Bhagoria, Anil Singh Yadav, (2013) has performed the numerical investigation on triangular rib solar air heater on CFD found that the maximum enhancement in the Nusselt number has been found to be 3.073 times over the smooth duct corresponds to relative roughness height (e/D) of 0.042 and relative roughness pitch (P/e) of 7.14 at Reynolds number (Re) of 15,000 in the range of parameters investigated.

Apurba Layek, Saini J.S., Solanki S.C., (2009) has performed the experimental investigation on solar air heater with chamfered rib-groove roughness on absorber plate. Ribs with chamfer angle 18 degree have the highest Nusselt number and Thermo-hydraulic performance factor in the range of 0 to 30 degree. The results obtained by experiments

were compared with square rib-groove roughness on absorber plate and with smooth duct.

III. METHODOLOGY

Governing equation of CFD is Navier's Stokes equation and based on conservation of mass, momentum and energy. The Navier-Stokes equations are vector equations, meaning that there is a separate equation for each of the coordinate directions.There are thus three different momentum equations that together comprise the Navier-Stokes Equations.

A. Pre-Processor

A pre-processor is used to define the geometry for the computational domain of interest and generate the mesh of control volumes (for calculations). Generally, the finer the mesh in the areas of large changes the more accurate the solution. Fineness of the grid also determines the computer hardware and calculation time needed. Design modeler and Mesh tool in ANSYS Workbench are used as pre-processor.

B. Solver

The solver makes the calculations using a numerical solution technique, which can use finite difference, finite element, or spectral methods. Most CFD codes use finite volumes, which is a special finite difference method. First the fluid flow equations are integrated over the control volumes (resulting in the exact conservation of relevant properties for each finite volume), then these integral equations are discretised (producing algebraic equations through converting of the integral fluid flow equations), and finally an iterative method is used to solve the algebraic equations.

C. Post-Processor

The post-processor provides for visualization of the results, and includes the capability to display the geometry/mesh, create vector, contour, and 2D and 3D surface plots. Particles can be tracked throughout a simulation, and the model can be manipulated (i.e. changed by scaling, rotating, etc.), and all in full coloured animated graphics. CFD Post is the post-processor used for this project.

A rectangular section is considered for analysis. It consisted of three sections, test section of length L_2 = 280 mm, entrance section of length L_1= 245 mm and exit length of length L_3 = 115 mm [1]. The domain on which numerical simulations are performed is two-dimensional.

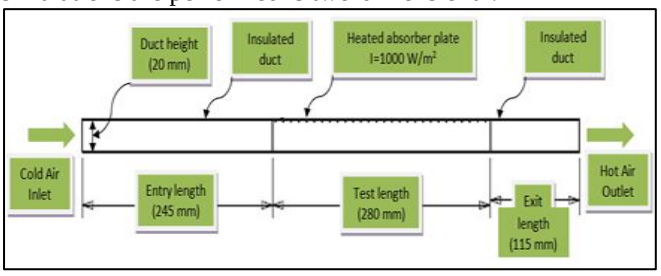

Fig. 2: Sketch of computational domain

Re is varied from 3800-18000 as this is the range in which solar air heaters particularly have higher efficiencies. Constant heat flux of value approximately 1000 W/m^2 was supplied only on the upper wall of the absorber plate. Simulations were performed assuming the flow to be steady.

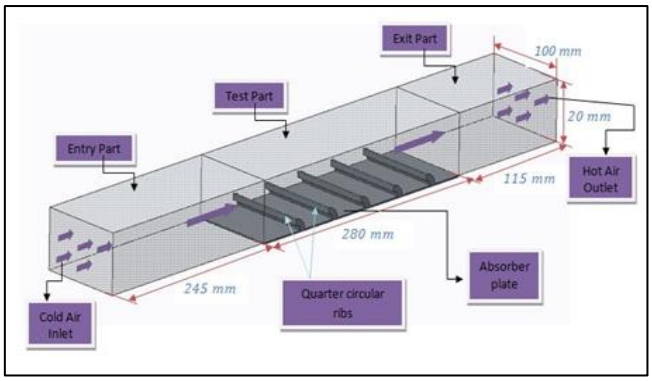

Fig. 3: 3-D geometry of solar air heater duct

2-Dimensional computational domain has been made using software, Creo Parametric. This model is then saved into IGES file format and is than imported into CFX 14. In ANSYS CFX geometry modeler, the model imported from Creo Parametric will have the same dimensions as that in Creo Parametric. Due to complexity in the designing of geometry, Creo Parametric has been used

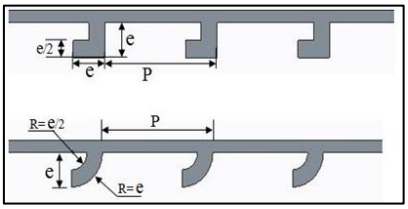

Fig. 4: L shape and quarter circle shape ribs

The meshing work was accomplished on commercially available ANSYS meshing software. The geometry created was imported in ANSYS meshing. The meshed domain consisted mostly of uniform sized cells as shown in Fig. 4.3. Fine meshing was completed near the absorber plate walls in order to solve the concerned governing differential equations accurately in the laminar sub-layers at these regions. The mesh size increased towards the center. The size of the grid was constant lengthwise in entrance and exit sections of the duct.

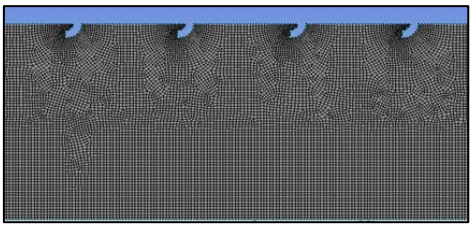

Fig. 5: Meshed model of quarter circle

D. Solution

The upwind scheme "second order upwind scheme" was selected for momentum and energy equations. In order to couple velocity and pressure, the SIMPLE algorithm was applied. Temporal discretization was achieved using the solution method "Implicit integration". Standard scheme was utilized to interpolate pressure and the relaxation factors for pressure, density, body forces, momentum and energy were maintained at 0.3, 1, 1, 0.7 and 1 respectively. A low convergence criteria of 10^{-6} was chosen for energy equation and 10^{-3} was chosen for continuity and velocity equation for the residuals in order to accurately predict different parameters.

E. Calculation of Nusselt number

1) Reynolds number

$$Re = \frac{\rho v D_h}{\mu}$$

2) Local heat transfer coefficient is

$$h_z = \frac{q''}{(T_w - T_f)}$$

3) Average heat transfer coefficient equation is

$$h_{avg.} = \frac{1}{L}\int_0^L h_z dz$$

During experimental methodology, a different method is adopted to measure the average heat transfer coefficient

$$h_{avg.} = \frac{\dot{m} C_p (T_o - T_i)}{A_p (T_{pm} - T_{fm})}$$

Where $T_{pm} = \frac{1}{N}\sum T_s$ and $T_{fm} = \frac{(T_i + T_o)}{2}$

4) Local Nusselt number

$$Nu_z = \frac{h_z D_h}{k}$$

5) Average Nusselt number

$$Nu_{avg} = \frac{h_{avg} D_h}{k}$$

F. Calculation of friction factor

The friction factor for rough surface is determined from the measured values of pressure drop across the test length:

$$f_r = \frac{(\Delta P) D_h}{2\rho_{air} L v^2}$$

ΔP is pressure drop in the duct,
ρ_{air} is density of air,
L is length of duct,
v is average velocity of air.

G. THPF

It is desirable that design of solar air heater should be made in such a way that it should transfer maximum heat energy to the flowing fluid with minimum consumption of pumping power. Thermal performance of a solar air heater concerns with the heat transfer process within the collector while hydraulic performance concerns with pressure drop in the duct. Therefore in order to analyze overall performance of a solar air heater, thermo-hydraulic performance factor should be evaluated by considering thermal and hydraulic characteristics of the absorber plate simultaneously.

Thermo-hydraulic enhancement factor:

$$THPF = \frac{(Nu_r/Nu_s)}{\left(\frac{f_r}{f_s}\right)^{1/3}}$$

IV. Results and Discussion

The CFD results are validated in the form of average Nusselt number and friction factor for smooth duct with the correlations proposed by Dittus-Boelter and Blasius. Comparison of CFD and correlation values of Nusselt number and friction factor is shown in Fig 5.1 and Fig 5.2. The CFD and correlations values are in good agreement to ensure the accuracy of the data being collected from the CFD results.

Nusselt number for smooth duct (Nu_s) is calculated by empirical correlation given by Dittus – Boelter,

$$Nu_s = 0.023\ Re^{0.8}\ Pr^{0.4}$$

Friction factor for smooth duct (f_s) can be calculated by correlation given by Blasius equation,

$$f_s = 0.0791\ Re^{-0.25}$$

S. No.	Reynolds number	Nu_s from Dittus-Boelter correlation	Nu_s from CFD results	Error (%)
1	3800	14.32	14.935	-4.118 %
2	5000	18.235	18.6	-1.962 %
3	8000	28.135	27.1	3.8192 %
4	12000	38.185	37.47	1.9082 %
5	15000	44.63	44.79	-0.357 %
6	18000	50.28	51.83	-2.991 %

Table 1: Nusselt number for smooth duct

S. No.	Reynolds number	f_s from Blasius correlation	f_s from CFD results	Error (%)
1	3800	0.010075	0.01082	7.394541
2	5000	0.00947	0.00988	4.329461
3	8000	0.00836	0.00869	3.947368
4	12000	0.00755	0.00799	5.827815
5	15000	0.00715	0.00765	6.993007
6	18000	0.00683	0.00732	7.174231

Table 2: Friction factor for smooth duct

S. No.	Rib geometry	P/e	Friction factor (f_r)					
			Re = 3800	Re = 5000	Re = 8000	Re = 12000	Re = 15000	Re = 18000
1	"Qc" rib	7.14	0.0351	0.0319	0.0286	0.0256	0.0241	0.0229
2		10.71	0.0319	0.0295	0.0265	0.0241	0.0228	0.0209
3		14.29	0.0293	0.0269	0.0236	0.0225	0.0217	0.0204
4	"L" rib	7.14	0.0328	0.0299	0.0264	0.0239	0.0224	0.0216
5		10.71	0.0303	0.0279	0.0247	0.0226	0.0212	0.0201
6		14.29	0.0281	0.0256	0.0227	0.0212	0.0204	0.0193

Table 3: Comparison of friction factor between "quarter circular" ribs and reverse "L" shaped ribs

S. No.	Rib geometry	P/e	Thermo-hydraulic performance factor (THPF)					
			Re = 3800	Re = 5000	Re = 8000	Re = 12000	Re = 15000	Re = 18000
1	"Qc" rib	7.14	1.9028	1.9546	1.9676	2.0162	2.0668	2.02919
2		10.71	1.8359	1.8771	1.8931	1.9343	1.9917	1.91849
3		14.29	1.7270	1.7670	1.7917	1.8273	1.9062	1.8178
4	"L" rib	7.14	1.8253	1.8628	1.8733	1.9052	1.9361	1.9080
5		10.71	1.7851	1.8144	1.8242	1.8559	1.8859	1.8352
6		14.29	1.6830	1.7124	1.7248	1.7564	1.8155	1.7618

Table 3: Comparison of friction factor between "quarter circular" ribs and reverse "L" shaped ribs

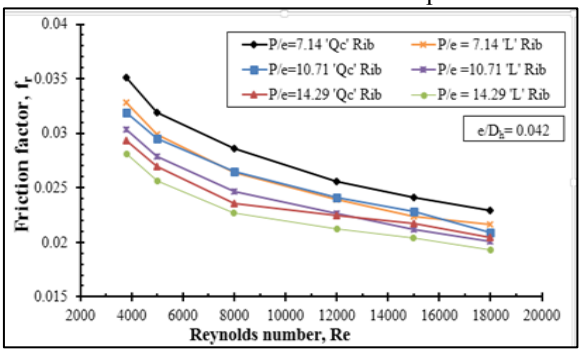

Fig. 6: Effect of rib geometry on friction factor

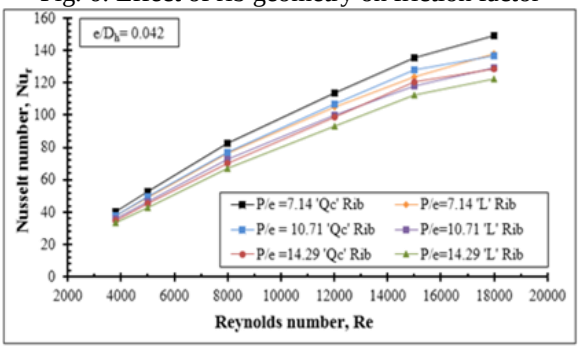

Fig. 7: Effect of rib geometry on nusselt number

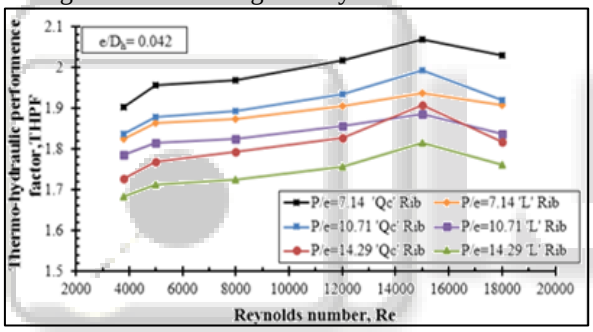

Fig. 8: Effect of rib geometry on nusselt number

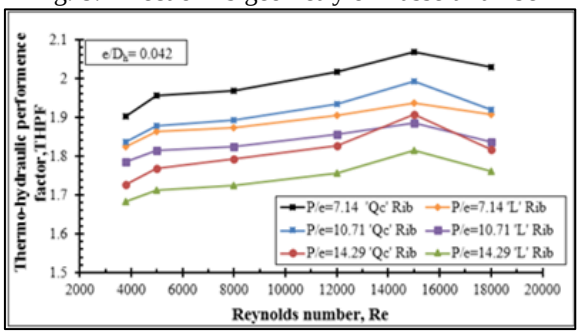

Fig. 9: Effect of rib geometry on thermo-hydraulic performance factor

As the Reynolds number increases roughness elements begin to project beyond the laminar sub-layer. Laminar sub-layer decreases with increase in Reynolds number. In addition to this there is local contribution to the heat removal by the vortices originating from ribs which increases heat transfer rate. This is because the ribs disturbs the development of boundary layer of fluid flow and increases the turbulent intensity caused by increase in turbulence dissipation rate and turbulence kinetic energy

V. CONCLUSION

A detailed study was undertaken to understand the mechanism and some significant parameters of solar air heater. Augmentation of heat transfer by using quarter circular ribs on inner surface of absorber plate was analyzed in detail. It has been seen that by changing the geometry of ribs from reverse L shape to quarter circular shape there is significant increase in friction factor. The reason behind this increment in friction factor was bigger vortex formation due to which pressure difference increased that means friction factor increased. Of course augmentation in friction factor is not good for overall performance of solar air heater but bigger vortex generation also helped air particles to absorb more heat from absorber plate that means it has been seen Nusselt number also increased to a great extent that cause increment in thermo hydraulic performance factor, THPF i.e. actually needed to achieve

1) Nusselt number increases for all cases with increase in Reynolds number in approximately similar manner with maximum values at P/e =7.14 and minimum values at P/e =14.29.
2) Nusselt number increases with decrease in relative roughness pitch (P/e) from P/e =14.29 to 7.14, but below P/e = 7.14 i.e. at P/e = 3.57, Nusselt number decreases because of entrapment of air flow between ribs due to which there is poor recirculation and reattachment of flowing fluid.
3) Maximum Nusselt number enhancement ratio (Nur/Nus) has been achieved 3.0298 for P/e =7.14 on Re = 15000.
4) It has been discovered from fig 5.4(a) and (b) that the percentage increment in Nusselt number with Reynolds number decreases with increase in Reynolds number.
5) Maximum percentage increase in Nusselt number has been recorded 56.31% from Re =5000 to 8000 for P/e =7.14
6) It can be seen there is sharp decrease in friction factor at initial range of Reynolds number, but by further increasing Reynolds number it would definitely attain an almost constant value.
7) Average friction factor tends to decrease as the Reynolds number increases for all cases as expected because of suppression of laminar sub-layer.
8) Maximum friction factor enhancement ratio (fr/fs) has been achieved 3.244 for P/e =7.14 on Re = 3800.
9) Friction factor increases with decreasing relative roughness pitch (P/e) upto P/e =7.14 as expected but by further decreasing the P/e value to 3.57, it has been seen that friction factor has been decreased due to entrapment of air particles between ribs which were not allowing the air particles for vortices formation that cause slight decrement in pressure drop and hence the friction factor decreased.
10) It can be observed that THPF increases with Reynolds number up to Re =15000 and then decreases for Re = 18000. This is due to, although Nusselt number is increasing with Reynolds number but friction factor will dominate the increase in Nusselt number after Re =15000.
11) Maximum THPF has been achieved 2.0668 for P/e =7.14 on Re = 15000.

12) The value of THPF increases with decrement in P/e value up to 7.14 after that due to entrapment of air between ribs it has been decreased.

VI. FUTURE SCOPE

1) Further investigation can be performed for various roughness design to get better performance of solar air heater.
2) Experimental studies with these variables will definitely refine the design of solar air heater.

REFERENCES

[1] Gupta D, Solanki S C, Saini J S; "Heated fluid flow in rectangular solar air heater ducts having transverse rib roughness on absorber plates." Solar Energy Vol. 61, No. 1, pp. 33-42 (1997).
[2] Bhagoria J L, Saini J S, Solanki S C; "Heat transfer coefficient and friction factor correlations for rectangular solar air heater duct having transverse wedge shaped rib roughness on the absorber plate." Renewable Energy 25 (2002) 341–369.
[3] Chaube A, Sahoo P K, Solanki S C; "Analysis of heat transfer augmentation and flow characteristics due to rib roughness over absorber plate of a solar air heater." Renewable Energy 31 (2006) 317–331.
[4] Karmare S V, Tikekar A N; "Analysis of fluid flow and heat transfer in a rib grit roughened -surface solar air heater using CFD"; International Journal of Heat and Mass Transfer 50 (2007) 4342–4351.
[5] Yadav A S, Bhagoria J L; "A CFD (computational fluid dynamics) based heat transfer and fluid flow analysis of a solar air heater provided with circular transverse wire rib roughness on the absorber plate"; Energy 55 (2013) 1127-1142.
[6] ANSYS Fluent 14.5. Documentation. Ansys, Inc; 2014.
[7] Anil Kumar, Man-Hoe Kim; "Effect of roughness width ratios in discrete multi V-rib with staggered rib roughness on overall thermal performance of solar air channel" Solar Energy 119 (2015) 399–414.
[8] Sukhmeet Singh, Bikramijit Singh, Hans V. S., Gill R.S.; "CFD (computational fluid dynamics) investigation on Nusselt number and friction factor of solar air heater duct roughened with non-uniform cross section transverse rib" Energy 84 (2015) 509e517

